NASA TECHNICAL MEMORANDUM

NASA TM X-71418

NASA TM X-71418

A MODEL FOR THE PRESSURE EXCITATION SPECTRUM AND ACOUSTIC IMPEDANCE OF SOUND ABSORBERS IN THE PRESENCE OF GRAZING FLOW

by Edward J. Rice
Lewis Research Center
Cleveland, Ohio

TECHNICAL PAPER proposed for presentation at
Aero-Acoustics Conference sponsored by the
American Institute of Aeronautics and Astronautics
Seattle, Washington, October 15 - 17, 1973

A MODEL FOR THE PRESSURE EXCITATION SPECTRUM AND ACOUSTIC IMPEDANCE OF SOUND ABSORBERS IN THE PRESENCE OF GRAZING FLOW

Edward J. Rice*
Lewis Research Center
National Aeronautics and Space Administration
Cleveland, Ohio

E-7656

Summary

The acoustic impedance of sound absorbers in the presence of grazing flow is essential information when analyzing sound propagation within ducts. A unification of the theory of the nonlinear acoustic resistance of Helmholtz resonators including grazing flow is presented. The nonlinear resistance due to grazing flow is considered to be caused by an exciting pressure spectrum produced by the interaction of the grazing flow and the jets flowing from the resonator orifices. With this exciting pressure spectrum the resonator can be treated in the same manner as a resonator without grazing flow but with an exciting acoustic spectrum.

One of the important implications of this model is that a multiple degree of freedom resonator can be analyzed with grazing flow. Using the grazing flow pressure spectrum, the nonlinear acoustic resistance can be properly distributed among the several elements of the resonator.

The development of the model is presented including both the determination of the exciting pressure spectrum and the nonlinear acoustic resistance derived from this spectrum. A comparison is made between the results of the impedance model and some experimental resistance data.

Introduction

The acoustic impedance of sound absorbers in the presence of grazing flow is essential information for the analysis or design of noise suppressors. This impedance is used as the boundary condition for sound propagation analysis.

The acoustic impedance of Helmholtz resonators is fairly well understood when there is no grazing flow. There is a small frequency dependent resistance component often referred to as the linear resistance. This is caused by the viscous scrubbing action of the fluid over the surfaces. With a high amplitude acoustic pressure there is another resistance component usually called the nonlinear acoustic resistance. This is caused by the viscous dissipation associated with the jets emanating from the orifices of the resonator[1]. Ingard[2] has shown experimentally that this nonlinear resistance is proportional to the peak magnitude of the orifice velocity. This proportionality has been shown analytically by Sirignano[3] and Zinn[4]. The velocity dependance of the acoustic resistance has been shown to hold instantaneously and has been used to calculate acoustic resistance with multiple frequency excitation[5].

However, when there is a grazing flow impressed upon the resonator the acoustic impedance is much more complicated and not well understood. Large nonlinear acoustic resistances have been demonstrated experimentally[6,7,8] even without high amplitude acoustic signals. At the grazing flow velocities encountered in typical turbofan ducts the acoustic resistance due to grazing flow completely dominates the other resistance phenomena, especially for perforated plate over honeycomb wall construction.

The grazing flow impedance has been handled in a completely empirical manner with a variety of approaches[5,8,9]. Little understanding has been obtained except that the acoustic amplitude and grazing flow effects seem to be additive. That is, the amplitude effects dominate at low grazing flow but are overcome by the grazing flow effects at high grazing flow velocities.

The purpose of this paper is to unify the theory of the nonlinear resistance of Helmholtz resonators. The basic hypothesis of the model is that the acoustic amplitude and grazing flow effects are manifestations of the same phenomena. The grazing flow effects can be handled in exactly the same way as the acoustic amplitude effect. It is hypothesized that the grazing flow interacts with the jets emanating from the resonator orifices to produce a spectrum of pressure perturbations at the orifice. This pressure perturbation spectrum excites the resonator in exactly the same way as an acoustic spectrum to produce oscillating flow within the orifices. This oscillating flow produces the nonlinear resistance which is proportional to the resultant root-mean-squared velocity.

Analytical Model

Excitation Pressure Spectrum

First the pressure excitation spectrum due to the interaction of the orifice jets and the steady grazing flow will be developed. The basic assumption is that pressure oscillations are produced within the potential core of the jet due to vortex shedding from the grazing flow over this core. Consider the model in Figure 1 where the potential core of the jet is shown penetrating into the grazing flow which has a velocity gradient as shown. It is assumed that the potential core of the jet acts somewhat like a solid body in a crossflow with vortices shed off the trailing side of the body. The frequency of this vortex shedding is assumed to be characterized by a local Strouhal number. The jet potential core is a cone and not a cylinder, but it might be thought of as being made up of a multitude of short cylinders which decrease in diameter away from the wall. Near the wall where the jet potential core diameter is largest and the velocity is low, low frequency vortex shedding will occur. Further out in the flow the jet diameter has decreased and the grazing flow velocity increased so that higher frequency shedding will occur.

*Aerospace Engineer, V/STOL & Noise Div, AIAA Member

The vortex shedding will cause pressure perturbations around the potential core. It is assumed that the pressure perturbation amplitude felt within the potential core at a distance y away from the wall can be given as (all symbols are defined in Appendix A):

$$P(y) = \tfrac{1}{2} C_D \rho V^2(y) \qquad (1)$$

where V(y) is the local grazing flow velocity in the boundary layer and C_D may be considered as an oscillatory drag coefficient which is to be determined empirically. These pressure oscillations at point y are assumed to occur at a frequency given by

$$f(y) = \frac{S\, V(y)}{d(y)} \qquad (2)$$

which is the usual type of Strouhal frequency relationship such as given by Roshko[10]. The Strouhal number S can be expressed as

$$S = \frac{0.212\ (Rey)^{3/2}}{270 + (Rey)^{3/2}} \qquad (3)$$

where

$$Rey = \frac{V(y)\, d(y)}{\nu} \qquad (4)$$

is the local Reynolds number at a distance y from the wall. Equation (3) was determined by fitting the data from reference 10. These data were taken with flow over cylinders, but they are assumed here to apply locally to the conical potential core. From equation (3) it is seen that for high Reynolds number, S = 0.212.

The pressure perturbation in the potential core must be converted to an oscillation at the orifice. It is assumed that this can be done by an inverse squared distance or area ratio relationship similar to that used in free field sound propagation. This is done by multiplying equation (1) by $(d(y)/do)^2$ to form

$$P_o(y) = \tfrac{1}{2} C_D \rho V^2(y) \frac{d^2(y)}{d_o^2} \qquad (5)$$

where $P_o(y)$ is the orifice pressure perturbation amplitude caused by vortex shedding at point y. The potential core diameter is assumed to vary as

$$d(y) = d_o - 2y \tan\alpha \qquad (6)$$

where α is the angle of the potential core erosion due to mixing. This angle is assumed to be seven degrees in all of the calculations which follow. This is the value found for the jet mixing angle of coaxial flow over a jet.

Response of Resonator to the Excitation Pressure Spectrum

Now that an oscillating pressure spectrum has been developed, the response of the Helmholtz resonator can be treated the same as in the case of no grazing flow but with an acoustic excitation spectrum.

The following equations determine the response of the resonator.

Resistance:

$$\theta = \frac{\sqrt{8\nu\omega}}{\sigma c}\left(1 + \frac{t}{d_o}\right) + 5.4\times10^{4}\mu t + \frac{V_o}{\sigma c} \qquad (7)$$

Reactance:

$$\chi = \frac{(t + \ell)\omega}{c} - \cot\left(\frac{\omega b}{c}\right) \qquad (8)$$

Orifice Velocity:

$$|V_o| = \sqrt{\sum_i (V_{oi})^2} \qquad (9)$$

where the orifice velocity at each selected frequency is

$$|V_{oi}| = \frac{|P_{oi}|}{\rho c \sigma (\theta_i^2 + \chi_i^2)^{\frac{1}{2}}} \qquad (10)$$

and $|P_{oi}|$ is the peak pressure amplitude at each frequency as determined by equations (2) and (5) due to the grazing flow. Equations (7) to (10) are usually thought to describe the behavior of the Helmholtz resonator without grazing flow. An additional empirical term is usually added to equation (7) to account for grazing flow. However, with the interpretation used in this paper these equations will handle grazing flow since the flow effect is introduced through P_{oi} in equation (10). Additional calculation considerations for the use of these equations are found in Appendix B.

The first two terms in equation (7) represent the linear resistance of the orifice (the second term requires t in feet); the first is a frequency dependent term while the second is a steady flow or low frequency limit term[5]. The third term represents the nonlinear resistance due to grazing flow and a high amplitude acoustic pressure spectrum. The orifice end correction (ℓ) in equation (8) is essentially zero[9] for the grazing flow velocities of usual interest. No attempt has been made here to treat the orifice end correction differently than in a previous empirical correlation[9]. It is possible that (ℓ) may be correlated with V_o in the future.

Equations (7) to (10) must be solved by iteration to obtain the resistance (θ) due to grazing flow. If there is an acoustic spectrum present, this can be considered simultaneously with the grazing flow pressure spectrum and each will contribute to the resistance depending upon their magnitude and frequency distribution.

Simplified Model

The following simplified expressions are presented only to give a qualitative picture of the principal variables involved in the analytical model. It is cautioned that these expressions are not good enough for serious calculations where the relations of the previous sections should be used.

Let the boundary layer be linear with a thickness δ and a velocity distribution be given by:

$$V(y) = \frac{V_\infty\, y}{\delta} \qquad (11)$$

Also let the oscillatory drag coefficient C_D be constant. Then using equations (6) and (11), equation (5) becomes

$$P_o(y) = \frac{C_D \rho V_\infty^2}{2\delta^2 d_o^2} y^2 (d_o - 2y \tan\alpha)^2 \quad (12)$$

This is the oscillatory pressure in the resonator orifice due to vortex shedding a distance y away from the wall. It is interesting to note what the peak of the frequency spectrum is. Since frequency is related to y through equation (2), equation (12) can be differentiated with respect to y to obtain the maximum pressure. When this is done the result is:

$$P_{o,max} \propto \rho V_\infty^2 \left(\frac{d_o}{\delta}\right)^2 \quad (13)$$

Now most of the response of the resonator (eq. (10)) occurs at the tuned points ($\chi = 0$). Assume that the peak pressure (eq. (13)) occurs at the tuned point (in any event the pressure at the tuned point is proportional to the peak). Then equation (10) becomes:

$$|V_{oi}| \propto \frac{\left(\frac{V d_o}{\delta}\right)^2}{\sigma C \theta_i} \quad (14)$$

Assume that the linear resistances in equation (7) are very small compared to the nonlinear resistance. Further assume that V_{oi} at the tuned point dominates V_o (eq. (9)), thus equation (7) becomes:

$$\theta = \frac{|V_{oi}|}{\sigma C} \quad (15)$$

Combining equations (14) and (15) (with $\theta = \theta_i$) there results

$$\theta \propto \frac{d_o V_\infty}{\sigma C \delta} \quad (16)$$

Thus the nonlinear acoustic resistance due to grazing flow increases with orifice diameter and grazing flow velocity but is reduced by increasing boundary layer thickness. This would imply that woven or sintered materials with very small hole sizes would have less grazing flow resistance than a typical perforated plate.

The above expression agrees qualitatively with the experimentally determined effect of the grazing flow velocity and boundary layer thickness on the acoustic resistance found in reference 6.

Comparison of Theory and Data

In all of the calculations which follow the complete model of equations (2) to (10) and the equations in Appendix B were used. Included herein is the determination of the functional form of C_D, a comparison for steady flow resistance and a comparison for specific acoustic resistance.

Empirical Determination of C_D

A wide variety of steady flow resistance data with grazing flow was studied to find the functional form of the oscillatory drag coefficient C_D in equation (5). These data included many grazing flow velocities, orifice diameters and open area ratios as well as boundary layer profiles with and without boundary layer trips. These data were supplied by The Boeing Company, Wichita, Kansas.

The theoretical model was exercised using a wide range of values for C_D in equation (5). The calculated values of resistance were compared to each experimental data point and the best value of C_D was determined. The best form of the oscillatory drag coefficient was found to be

$$C_D = k\sqrt{\frac{d(y)}{V(y)}} \quad (17)$$

where k is a constant which will be determined in the next two sections for steady flow and acoustic resistance calculations. It is interesting to note that by use of equation (2), equation (17) can be expressed as

$$C_D = k\sqrt{\frac{S}{f(y)}} \quad (18)$$

Thus C_D is a function only of the local pressure perturbation frequency due to the vortex shedding from the potential core of the jet.

Steady Flow Resistance Comparison

The steady flow resistance data mentioned above (from The Boeing Co., Wichita, Kansas) was obtained by measuring the steady-flow pressure drop (ΔP) and flow velocity (V_a) through the array of orifices. These measurements were obtained for a variety of perforated plate samples in the presence of several grazing velocities. The resistance values used were for vanishingly small steady flows so that the flow would not influence the resistance. The calculated values of resistance include only the second and third terms of equation (7) (not frequency dependent) since only the steady flow resistance is considered here.

The comparison of the experimental and calculated steady flow resistances are shown in Figure 2. The solid symbols represent data taken with a 3/16 inch boundary layer trip. The boundary layer profiles provided with the data were simulated in the theoretical calculations. The calculated values are seen to compare quite well with the experimental data.

The value of k used in equation (17) was 14.0. This value may seem quite large until it is recalled that $d(y)/V(y)$ is quite small, and the resultant C_D values are thus quite moderate.

Specific Acoustic Resistance Comparison

For comparisons with specific acoustic resistance data, all of the terms in equation (7) were used for the theoretical resistance calculations. The same functional form of C_D given by equation (17) was used with only a small change made in the value of k.

Some acoustic resistance data along with representative boundary layer profiles are given in reference 8. There was considerable scatter in these data, and average values were used. These data are compared to the theoretical calculations in Figure 3. The agreement is seen to be excellent

for four of the five samples. No satisfactory explanation can be given at this time for the disagreement of the theory with this single liner sample.

The value of k used for the comparisons of Figure 3 was 11.5. Although this differs slightly from the value used with steady flow impedance (14.0), it is not unusual that these two somewhat different phenomena (steady flow and acoustic resistance) would require such a difference.

Sample Excitation Pressure Spectra

One of the ways in which this model can be checked and possibly altered is to measure the excitation pressure spectrum which is impressed upon the orifice of the resonator. Plans have been made to provide this experimental check. It is thus interesting to look at some excitation pressure spectra to see what the model, as presently constituted, would predict.

In all of the pressure spectra which follow, equation (5) was used to calculate the pressure amplitude and equation (2) was used to calculate the frequency. This was accomplished by varying the distance from the wall (y) in both equations. Equations (3), (4), and (6) were used in the process along with a 1/7 power velocity profile.

In Figure 4 the spectrum levels are given for three different velocities with only a slight variation in boundary layer thickness. The slight change in δ was due to making the calculations at the same axial distance from the beginning of boundary layer build up, and δ is a weak function of V_∞. Note that these spectrum levels are based on a per frequency normalization and must be integrated to generate more common forms such as 1/3 octave spectra.

The low frequency portions of the spectra in Figure 4 are seen to be coincident for all three grazing flow velocities. The spectrum level peaks at a frequency which appears to be proportional to grazing flow velocity and then falls off. It would be more satisfying to see the spectrum level lower at all frequencies for V_∞ = 100 fps than for 600 fps. The spectra in Figure 4 indicate that essentially all of the difference in nonlinear acoustic resistance due to grazing flow would be controlled by the resonator response at the second and third tuned frequencies ($\approx$ 8000 and 14,000 Hz). Essentially no difference would be caused by the response at the first tuned frequency of 2500 Hz.

In Figure 5 spectrum levels are presented for differing boundary layer thicknesses at a constant grazing flow velocity. Again the low frequency parts of the spectra are coincident. The change in nonlinear acoustic resistance due to grazing flow will be controlled by the third tuned frequency at 14,000 Hz.

The accuracy of the spectra presented above cannot be judged at this time. Detailed pressure spectra measurements will be needed to check the model.

Concluding Remarks

The important point in this paper is that the nonlinear acoustic impedance due to grazing flow may be able to be treated in exactly the same way as a high amplitude acoustic spectrum without grazing flow. An important implication of this approach is that complex acoustic liner constructions, such as double or multiple degree of freedom acoustic liners, can easily be analyzed with grazing flow. Once the pressure spectrum due to grazing flow is established the complex liner can be analyzed with the nonlinear acoustic resistance properly distributed among the several flow paths within the liner.

This paper must be considered as just a start in understanding the fundamentals of the grazing flow impedance. Some of the basic assumptions of the model must be checked experimentally. The spectrum of the exciting pressure in the orifices must be measured to determine if the development of the spectrum through equations (1) to (6) is indeed reasonable. Some modifications of the approach will no doubt be necessary after careful study of data.

Several other questions may arise in regard to this model. How does the orifice jet flow get started so that the jet-grazing flow interaction pressure spectrum can get established and ultimately dominate the impedance? Any disturbance can trigger the flow in the resonator just as noise or transients can trigger an electric oscillator. The wall pressure fluctuations due to the boundary layer as shown by Bull[11] can easily start the process. However, these pressure fluctuations alone are not high enough to explain the magnitude of the grazing flow resistance. Also it can be shown that the standard pressure spectrum due to the boundary layer provides a dependence upon boundary layer thickness which is inverse to the experimentally measured acoustic resistance dependence. The model of this paper has been shown to have the proper qualitative dependence upon boundary layer thickness (eq. (16)).

A second question occurs in that the jet flow is not always out of the orifice as shown in Figure 1 but is flowing into the orifice half of the time. During this inflow probably the only pressures on the orifice are the standard random spectrum due to the boundary layer and possibly pressure fluctuations due to separations and impingement on the orifice edges. The solution for the exciting spectrum in the actual case of alternating flow direction would indeed by very difficult, and it is hoped that this added complication can be adequately handed by the empirical determination of C_D in equation (17).

A more sophisticated approach to the erosion of the potential core of the jet might also be tried. The erosion angle α is probably a function of several variables including jet velocity and the boundary layer profile. However, this is probably not worthwhile since it was found that most of the exciting pressure spectrum of consequence is produced very near the wall and is more a function of the initial jet diameter and the boundary layer profile than the erosion angle.

The model does provide an adequate explanation for most of the available grazing flow acoustic resistance data. It is hoped that this model will provide a beginning for the better understanding of the physics of the problem.

References

1. Ingard, Uno, and Labate, S., "Acoustic Circulation Effects and the Nonlinear Impedance of Orifices," J. Acoust. Soc. Am., Vol. 22, No. 2, Mar. 1956, pp. 211-218.

2. Ingard, Uno, and Ising, H., "Acoustic Nonlinearity of an Orifice," J. Acoust. Soc. Am., Vol. 42, No. 1, 1967, pp. 6-17.

3. Sirignano, W. A., and Tonon, T. S., "Nonlinear Aspects of Combustion Instability in Liquid Propellant Rocket Motors," CR-72426, June 1968, NASA.

4. Zinn, B. T., "A Theoretical Study of Nonlinear Damping by Helmholtz Resonators," Paper 69-481, 1969, AIAA.

5. Rice, E. J., "A Model for the Acoustic Impedance of a Perforated Plate Liner with Multiple Frequency Excitation," Presented at Acoustical Soc. Am. meeting Denver, Oct. 1971; Also NASA TM X-67950.

6. Feder, E., and Dean, L. W., "Analytical and Experimental Studies for Predicting Noise Attenuation in Acoustically Treated Ducts for Turbofan Engines," CR-1373, 1969, NASA.

7. Budoff, M., and Zorumski, W. E., "Flow Resistance of Perforated Plates in Tangential Flow," TM X-2361, Oct. 1971, NASA.

8. Armstrong, D. L., "Acoustic Grazing Flow Impedance Using Waveguide Principles," CR-12048, Dec. 1971, NASA.

9. Rice, E. J., Feiler, C. E., and Acker, L. W., "Acoustic and Aerodynamic Performance of a 6-Foot Diameter Fan for Turbofan Engines. Part III. Performance with Noise Suppressors," TN D-6178, Feb. 1971, NASA.

10. Roshko, A., "On the Development of Turbulent Wakes from Vortex Streets," Report 1191, 1954, NACA.

11. Bull, M. K., "Boundary Layer Pressure Fluctuations," in Noise and Acoustic Fatigue in Aeronautics, edited by Richards, E. J., and Mead, D. J., John Wiley and Sons Ltd., 1968, pp. 169-180.

Appendix A -- Symbols

b	resonator cavity depth
c	speed of sound
C_D	oscillatory drag coefficient (see eq. (1) and (17))
$d(y)$	jet core diameter, shown as function of y
d_o	resonator orifice diameter
f	frequency
$f(y)$	frequency of pressure perturbations at a distance y from the wall (eq. (2))
k	empirical constant (see eq. (17))
ℓ	orifice and correction
$P(y)$	pressure perturbations in the jet core at y
$P_o(y)$	pressure perturbations at the orifice due to $P(y)$
P_{oi}	pressure perturbations at the orifice at the i^{th} frequency of the excitation spectrum
$P_{o,max}$	the peak of the pressure excitation spectrum
ΔP	steady flow pressure drop across an array of orifices
Re_y	Reynolds number (see eq. (4))
S	Strouhal number (see eq. (2))
t	orifice length
$V(y)$	grazing flow velocity at a distance y from the wall
V_a	steady flow velocity through an array of orifices
V_∞	grazing flow velocity far from the wall
V_o	rms orifice velocity
V_{oi}	orifice velocity at the i^{th} excitation frequency
$V_{oi,eff}$	effective orifice velocity at the i^{th} excitation frequency
X_i	maximum orifice fluid displacement at the i^{th} frequency
y	distance away from the liner
α	jet core erosion angle
δ	boundary layer thickness
θ	specific acoustic resistance
θ_i	specific acoustic resistance at the i^{th} excitation frequency
μ	dynamic viscosity
ν	kinematic viscosity
σ	open area ratio (orifice area to wall area)
χ	specific acoustic reactance
χ_i	specific acoustic reactance at the i^{th} excitation frequency
ω	angular frequency

Appendix B
Additional Calculation Considerations

Several more detailed considerations were deferred from the previous discussions to keep the development as uncomplicated as possible. These considerations will now be discussed.

Effect of Orifice Fluid Displacement

It was shown in reference 5 that at high frequencies the acoustic resistance was less than that predicted on the basis of peak orifice velocity (e.g., eq. (7)). This was interpreted (in ref. 5) as being due to the small orifice fluid displacement at high frequencies. If the displacement is small a jet will not fully form and the energy dissipation and thus the resistance will be decreased. This phenomenon can be handled in the following way by the use of an effective orifice velocity. Let

$$V_{oi,eff} = V_{oi}\, e^{-\left(\frac{d_o}{X_i}\right)^2} \qquad (B1)$$

where X_i is the maximum displacement of the orifice fluid at the i^{th} frequency. If the fluid displacement is large compared to the orifice diameter then

$$V_{oi,eff} \approx V_{oi} \qquad (B2)$$

but if $X_i \ll d_o$ then

$$V_{oi,eff} \approx 0 \qquad (B3)$$

For a sinusoidal oscillation,

$$|X_i| = \frac{V_{oi}}{\omega} = \frac{V_{oi}}{2\pi f} \qquad (B4)$$

Thus equation (B2) can be converted to

$$V_{oi,ef} = V_{oi}\, e^{-\left(\frac{2\pi f d_o}{V_{oi}}\right)^2} \qquad (B5)$$

This approach provided a very good fit to the acoustic resistance data in reference 5.

Interpolation of Velocity Response Between Incremental Frequencies

The velocity response of the resonator is seen to be a function of the resistance and reactance (eq. (10)). This response is greatest at the tuned frequencies ($\chi_i = 0$). Since the increments in frequency could not easily be selected to ensure hitting all of these tuned points (χ changes very rapidly with frequency at the higher tuned points as can be seen by a plot of eq. (8)), an interpolation procedure was devised to ensure inclusion of the effects of these points.

A velocity squared term integrated over each frequency increment is required in equation (9) so that an overall root-mean-squared velocity can be calculated to represent the effect of the entire pressure spectrum. If none of the terms on the right side of equation (10) vary rapidly with frequency over the frequency increment of interest, then equation (10) can be used directly in equation (9). The pressure and resistance can be safely assumed constant over a reasonably small frequency increment but the change in reactance must usually be considered.

By squaring and then averaging equation (10) through integration (and dropping the i subscript for convenience) the following results:

$$V_o^2 = \left(\frac{P_{oi}}{\rho c \sigma}\right)^2 \frac{\int_{f_1}^{f_2} \frac{df}{(\theta^2 + \chi^2)}}{(f_2 - f_1)} \qquad (B6)$$

The reactance (χ) can be represented sufficiently accurately by a linear Taylor expansion around $f = f_o$ by,

$$\chi = \chi_o + \left(\frac{\partial \chi}{\partial f}\right)_o (f - f_o) \qquad (B7)$$

where χ_o and $(\partial \chi / \partial f)_o$ are determined from equation (8) at $f = f_o$ (and using $\omega = 2\pi f$). By using equation (B7) in equation (B6) the resulting integral can be integrated in closed form and equation (B6) becomes:

$$V_o^2 = \left(\frac{P_o}{\rho c \sigma}\right)^2 \frac{\left[\arctan\left(\frac{\chi_2}{\theta}\right) - \arctan\left(\frac{\chi_1}{\theta}\right)\right]}{\theta (f_2 - f_1)\left(\frac{\partial \chi}{\partial f}\right)_o} \qquad (B8)$$

where

$$\chi_2 = \chi_o + \left(\frac{\partial \chi}{\partial f}\right)_o (f_2 - f_o) \qquad (B9)$$

and

$$\chi_1 = \chi_o + \left(\frac{\partial \chi}{\partial f}\right)_o (f_1 - f_o) \qquad (B10)$$

If the slope of reactance with frequency $(\partial \chi / \partial f)_o$ is very small equation (B8) can be shown to approach the square of equation (10). Equation (B8) was used for all of the calculations presented in this paper.

Summary of Calculation Procedure

Since the equations are numerous and further complicated by an iteration procedure, a summary of the calculation procedure may be helpful.

First the excitation pressure spectrum due to grazing flow is established for the particular acoustic liner and boundary layer profile under consideration. A series of small steps away from the liner wall are selected (several values of y). At these several values of y the pressure amplitude (eq. (5)) and frequency (eq. (2)) are calculated. Equations (3), (4), and (6) and of course the desired boundary layer velocity profile are used in this process. The excitation pressure spectrum terms (P_{oi} in eq. (10)) due to grazing flow are now established. The acoustic pressure spectrum can now be added to the P_{oi} if this is desired.

Next the response of the resonator to the excitation pressure spectrum must be determined. This is done by using equations (7) to (10) and (B5). Recall that equation (B8) is an alternate to equation (10) which provides an interpolation between the finite number of frequencies.

The reactance (χ_i) at each frequency can be calculated immediately from equation (8). A dilemma occurs with equations (7), (9), and (10) in that acoustic resistance cannot be calculated until the rms velocity is determined, and the rms velocity cannot be determined until the resistance at each frequency is know. This clearly calls for an iteration procedure.

1. Assume a value of $|V_o|$; V_∞ would be a good start.

2. Calculate the resistance at each frequency from equation (7).

3. Calculate the orifice velocity at each frequency ($|V_{oi}|$) from equation (10), or alternately and perferably from equation (B8). Recall that the i subscript has been omitted from equation (B8) for brevity.

4. Correct each orifice velocity for the orifice fluid displacement effect by using equation (B5) which will give the effective orifice velocities.

5. Use the effective orifice velocities in equation (9) to calculate the root-mean-squared velocity ($|V_o|$) for the entire spectrum.

6. Compare $|V_o|$ with that assumed in step 1. It will be too small in the first iteration cycles. Reduce the assumed $|V_o|$ in step 1 and repeat all steps until the assumed and calculated $|V_o|$ agree. Interpolation can be used in the final steps of the iteration to speed up convergence. After convergence is obtained the desired values of resistance are calculated from equation (7).

The above procedure may seem lengthly but it is a simple job when performed on a computer.

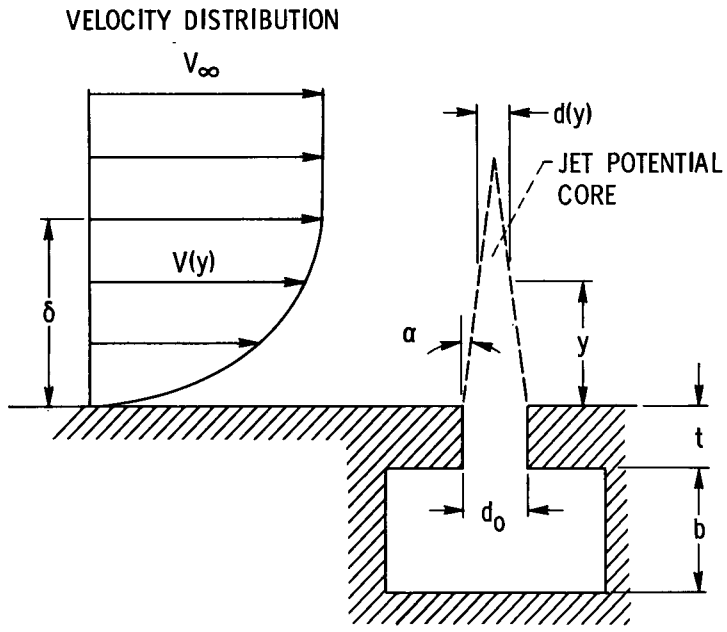

Figure 1. - Geometry used in analytical model.

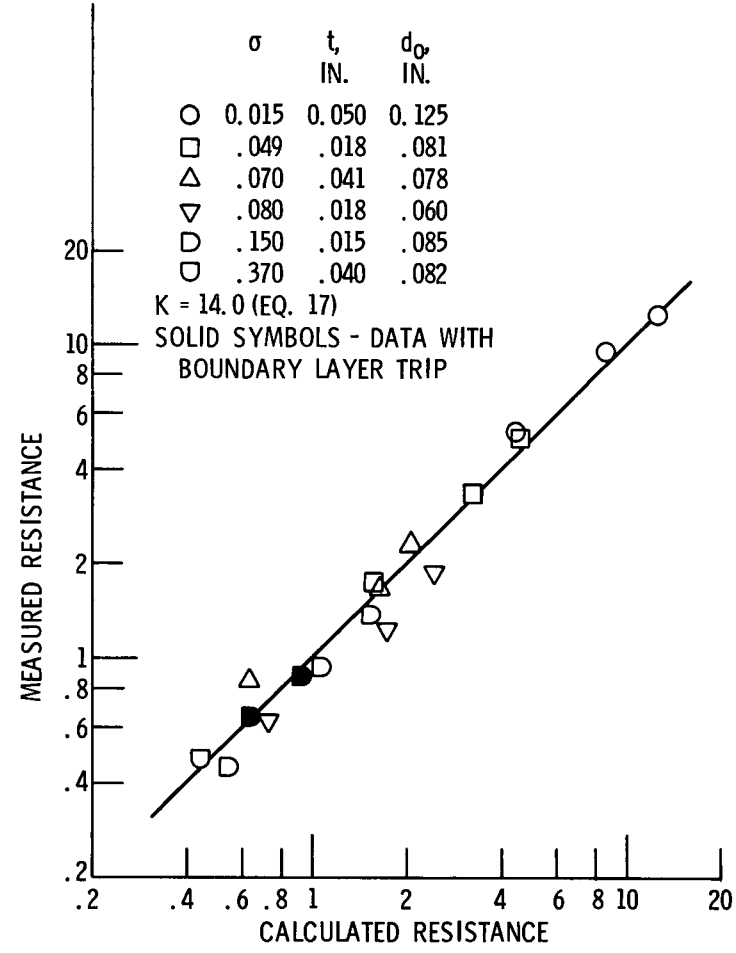

Figure 2. - Comparison of experimental and calculated steady flow resistance ($\Delta P/\rho CV_a$).

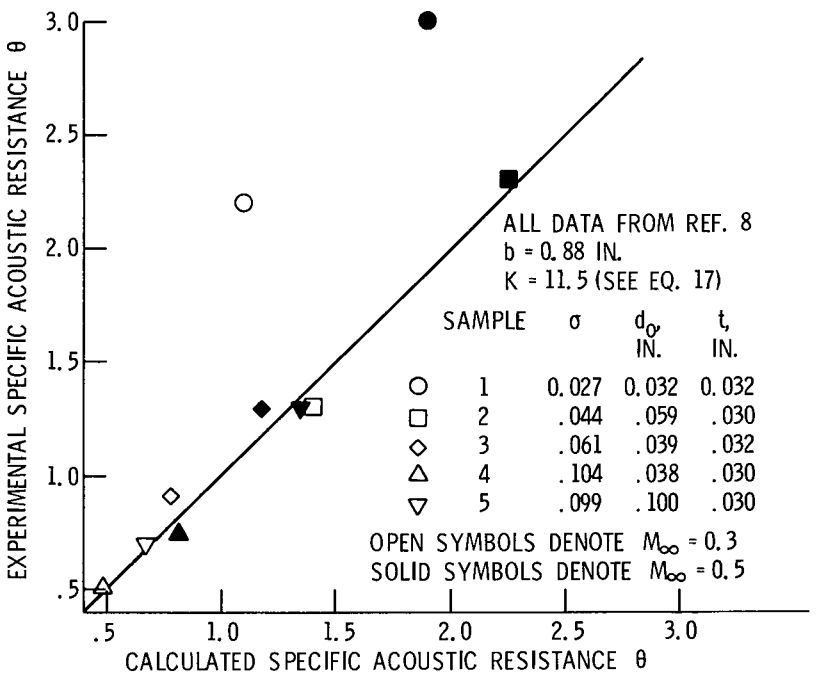

Figure 3. - Comparison of experimental and calculated acoustic resistance.

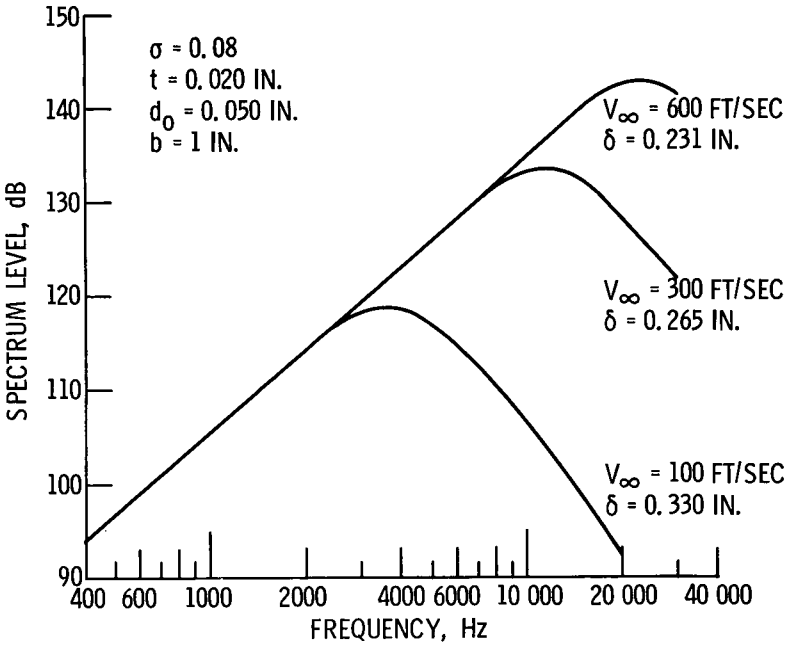

Figure 4. - Variation of excitation pressure spectrum level with grazing flow velocity.

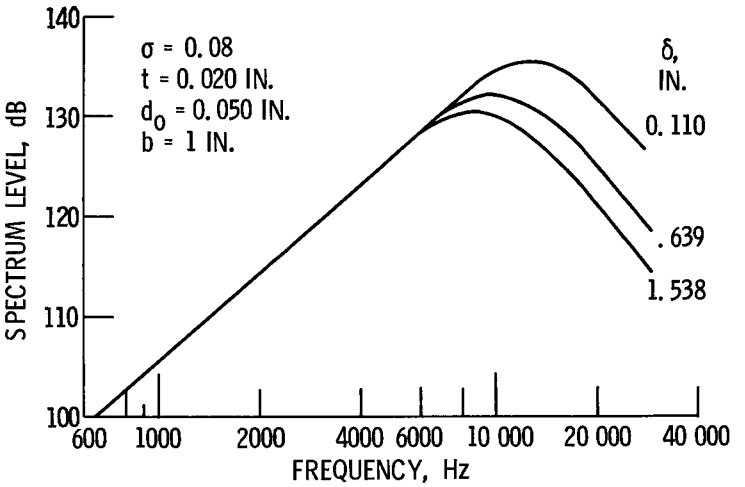

Figure 5. - Variation of excitation pressure spectrum level with boundary layer thickness for V_∞ = 300 ft/sec.